Australian Government
Department of Defence
Defence Science and
Technology Group

Recent Advances in Source Localization Using Range Measurements

Hatem Hmam and Kutluyil Dogancay

Cyber and Electronic Warfare Division
Defence Science and Technology Group

DST-Group-TR-3158

ABSTRACT

In this report we review and present a performance comparison of a number of recently proposed range-based source localization algorithms that approximate the maximum likelihood estimator. Although most of these algorithms are available in the literature we give an elaborated presentation of them and provide some comments on their performances. The optimization techniques used in these localization methods range from convex relaxation, global continuation to the generalized trust region subproblem method. Among the localization algorithms considered, the range weighted squared range least squares estimator (RW-SRLS) seems to be a particularly attractive algorithm as it is fast and yet only marginally suboptimal in a maximum likelihood sense, especially for small range measurement errors.

Published by

Cyber and Electronic Warfare Division
Defence Science and Technology Group
PO Box 1500
Edinburgh South Australia 5111 Australia

Telephone: 1300 333 362
Fax: (08) 7389 6567

AR-016-408
October 2015

APPROVED FOR PUBLIC RELEASE

Recent Advances in Source Localization Using Range Measurements

Executive Summary

In this report we review and present a performance comparison of a number of recently proposed range or time of arrival (TOA)-based source localization algorithms that approximate the maximum likelihood estimator. Some of these algorithms are available in the literature and others are contributed for the first time in this report. This comparison study is important because TOA-based geolocation is gaining popularity, mainly because of the steady emergence of more stable and accurate time clocks, which enable dispersed platforms/vehicles/soldiers to instantly deduce separation distances from signal flight times. A unit is then able to rapidly self-localize in difficult environments using as little as two or three time/position stamped signals (i.e. transmit time and position information is included in the signal's preamble).

Authors

Hatem Hmam
Cyber and Electronic Warfare Division

Hatem Hmam received his M.S. degree from the University of Houston, Texas, in 1988, and his Ph.D. degree in electrical engineering from the University of Cincinnati, Ohio, in 1992. He joined the Defence, Science and Technology Organization (DSTO, Australia) in late 1996 and is currently a senior research scientist in the Cyber and Electronic Warfare Division. His current research interests include emitter passive localisation and signal processing.

Kutluyil Dogancay
Cyber and Electronic Warfare Division

Kutluyil Dogancay received the BS degree with honours in electrical and electronic engineering from Bogazici University, Turkey, in 1989, the MSc degree in communications and signal processing from the University of London in 1992, and the PhD degree in telecommunications engineering from The Australian National University in 1996. During his postgraduate studies he was a recipient of the British Council scholarship, OPRS (overseas postgraduate research scholarship) and the ANU PhD scholarship. Since November 1999 he has been with the School of Engineering, University of South Australia, where he is currently an associate professor. He is also the Assistant Dean of Research Education for the Division of Information Technology, Engineering and the Environment.

Contents

This page is intentionally blank

1. Introduction

The passive localization of emitters is of considerable interest in many applications including defence, wireless communications and navigation. A number of localization techniques were proposed in the past depending on the type of measurements and position estimation approach. Most popular among these are the time of arrival (TOA), time difference of arrival (TDOA) and angle of arrival (AOA) localization algorithms (see, e.g., [1,2,3,4,5,6]).

In this paper we focus on range-based localization techniques in the plane which underpin TOA localization and are extensively utilised in sensor network localization. In particular we compare a number of advanced source location estimators and examine how closely they approximate the least squares estimator. The difference between these estimators is either the objective function or the computation method used to minimise it. The two most popular cost functions considered in the literature are the range least squares (R-LS) and the squared range least squares (SR-LS) [3]. The R-LS-based formulation is of great interest and has been known for its optimal performance [3][7]. If the measurement errors are zero-mean Gaussian, then it coincides with the maximum likelihood estimator (MLE). The main challenge is how to efficiently compute an R-LS position estimate.

A number of optimization tools may be applied to globally solve the R-LS problem and are usually computationally intensive. Polynomial continuation methods [8] or computer algebra techniques [9][10] can determine the global minimiser after transforming the R-LS problem into a system of multivariate polynomial equations. Other solution methods are based on semidefinite relaxation (SDR) [7][11][12][13] or polynomial optimization (POP) [14]. They can approximate the R-LS estimator to an arbitrary degree but at the expense of a significant increase in computer processing and memory storage. Another approach to address the R-LS problem is to apply a smoothing kernel to the LS cost function and progressively minimise it by continuation [15][16].

In the first part of the paper we present source localization approaches based on squared range measurements. The SR-LS source position estimator analysed in [3], is one classic estimator, which exhibits several nice mathematical properties. The position estimate can be computed exactly and efficiently using generalized trust region subproblem (GTRS) optimization techniques [17][18][19]. However, as we shall see later in the paper, the estimator is not optimal in the maximum likelihood sense [3]. We propose a variant of this estimator which uses range-based corrective weights to reduce the position estimation bias error. Most importantly the computational efficiency of this variant estimator, which we call range weighted SR-LS (RW-SRLS), is the same as that of the SR-LS [3]. Computer simulations of the

RW-SRLS estimator show definite advantages in terms of position accuracy and low computational effort.

In the second part of this paper we briefly present and compare the performance of some of the algorithms known to solve or best approximate the R-LS estimator. These include two contributions based on computer algebra and convex relaxation. The earliest research effort to mathematically approximate the R-LS solution was made by Cheung et al. [7]. Their proposed approximation method is a straightforward convex relaxation of the R-LS problem. Further work in [3] provided a rigorous analysis of their algorithm. As demonstrated in [3] its performance is often degraded because the relaxation solution can be significantly different from that of the original R-LS problem. An alternative relaxation formulation, called CPNBSP-SDR, is proposed in this paper, which shows improved performance accuracy. This work is related to that of [13] and both are computationally more efficient than the SLCP positioning method [12], which is restricted to two-dimensional geolocation problems. We next investigate the kernel continuation method of [16], which offers some performance compromise by using a smoothing parameter to control the shape of the cost function and progressively steer the solution towards the global minimum. However, it remains unclear how to update the smoothing parameter and a global convergence certificate is not provided. Furthermore the continuation derivations in [16] are only applicable to source localization problems in the plane. Finally we provide an algorithm which solves the R-LS problem exactly subject only to numerical round-off errors. This algorithm is based on the work [10] and transforms the problem of solving a multivariate polynomial system into the null space analysis of a large sparse matrix whose nonzero entries consist of shifted polynomial coefficients. This method, however, is suitable for smaller localization problems in the plane as it becomes computationally prohibitive when the number of measurements increases beyond three.

This report comprises a number of sections. Section 2 introduces the R-LS problem and provides some basic results related to the CRLB and the regional bound for the R-LS solution. The rest of the report is mainly divided into two parts where the first covers two variants of the SR-LS approach (Section 3). The second part (Sections 4 and 5) covers R-LS relaxation and continuation based source localization approaches. Section 6 presents Reid and Zhi's null space method to solve the R-LS problem exactly. Section 7 presents several important results highlighting performance comparisons among various source position estimators. Finally concluding remarks are made in Section 8.

2. Problem Formulation and Basics

2.1 Problem Formulation

In this subsection we introduce the source localization problem to be solved. Unless specifically mentioned we express the source localization problem in $\Re^n$, where $n=2$ and $n=3$ refer to source geolocation in the plane and in space, respectively. As will become clear later on, some localization algorithms are applicable to both $\Re^2$ and $\Re^3$, while others are only applicable in $\Re^2$. However, all computer simulation results are restricted to $\Re^2$. If we assume that the range measurement errors are independent zero-mean Gaussian, then the maximum likelihood (ML) source position estimator reduces to the nonlinear LS problem, which is denoted by R-LS as given in [3]

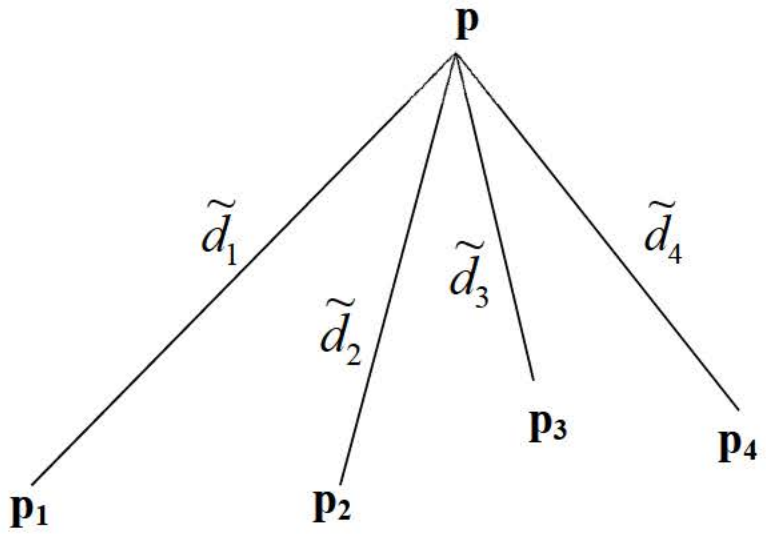

Figure 1: Emitter-receiver geometry. The emitter is at an unknown position, $\mathbf{p}$, to be estimated given measurements of the distances separating it from the sensors.

$$\min_{\mathbf{p}} \quad f(\mathbf{p}) = \sum_{i=1}^{N} w_i \left(\|\mathbf{p} - \mathbf{p}_i\| - \tilde{d}_i \right)^2 \tag{1}$$

As illustrated in Figure 1, the points, $\mathbf{p}_i$, are the known positions of N sensors in $\Re^n$ and $\tilde{d}_i$ their associated measured ranges to the source location. The non-negative numbers, w_i, are positive normalized weights (i.e. $\sum_{i=1}^{N} w_i = 1$). The weights are usually set proportional to the reciprocal of respective range measurement

error variances. For a localization problem in the plane (i.e. $n=2$), the coordinates of the source position, $\mathbf{p}$, are denoted as $(x, y)^T$. They become $(x, y, z)^T$ for a localization problem in space (i.e. $n=3$).

Before reviewing a number of range-based source localization works, we first establish a bound for the solution of (1).

2.2 Basic Results

The gradient at a minimum of (1) vanishes leading to

$$\nabla_{\mathbf{p}} f(\mathbf{p}) = \sum_{i=1}^{N} w_i \left(\mathbf{p} - \mathbf{p}_i - \tilde{d}_i \mathbf{u}_i\right) = 0 \tag{2}$$

where $\mathbf{u}_i = \dfrac{\mathbf{p} - \mathbf{p}_i}{\left\|\mathbf{p} - \mathbf{p}_i\right\|}$ is a unit direction vector pointing from the i[th] sensor position to $\mathbf{p}$. Expanding (2) leads to

$$\mathbf{p} = \sum_{i=1}^{N} w_i \left(\mathbf{p}_i + \tilde{d}_i \mathbf{u}_i\right) \tag{3}$$

If we let $\mathbf{p}_c = \sum_{i=1}^{N} w_i \mathbf{p}_i$, to be the sensor position centroid, then (3) reduces to

$$\mathbf{p} = \mathbf{p}_c + \sum_{i=1}^{N} w_i \tilde{d}_i \mathbf{u}_i \tag{4}$$

The next theorem shows that $\mathbf{p}$ is confined within the ball,

$$B_{\mathbf{p}_c, R} = \left\{\mathbf{p} \in \Re^n, \left\|\mathbf{p} - \mathbf{p}_c\right\| \le R\right\} \tag{5}$$

where $R = \sum_{i=1}^{N} w_i \tilde{d}_i$.

Theorem 1: An optimal solution, $\mathbf{p}$, of (1) is bounded within a ball centred at $\mathbf{p}_c = \sum_{i=1}^{N} w_i \mathbf{p}_i$ and of radius $R = \sum_{i=1}^{N} w_i \tilde{d}_i$.

Proof:

Let $\mathbf{p}_c = \sum_{i=1}^{N} w_i \mathbf{p}_i$ be the sensor centroid position. From (4) an optimal solution to (1) must satisfy $\mathbf{p} - \mathbf{p}_c = \sum_{i=1}^{N} w_i \tilde{d}_i \mathbf{u}_i$. If we apply the Euclidean norm to both sides of this equation, we obtain $\left\|\mathbf{p} - \mathbf{p}_c\right\| = \left\|\sum_{i=1}^{N} w_i \tilde{d}_i \mathbf{u}_i\right\|$ resulting in $\left\|\mathbf{p} - \mathbf{p}_c\right\| \le \sum_{i=1}^{N} w_i \tilde{d}_i \left\|\mathbf{u}_i\right\| = \sum_{i=1}^{N} w_i \tilde{d}_i$. This means that $\mathbf{p}$ belongs to the ball $B_{\mathbf{p}_c, R} = \left\{\mathbf{p} \in \Re^n, \left\|\mathbf{p} - \mathbf{p}_c\right\| \le R\right\}$. □

Finally the error performance of all geolocation estimators needs to be assessed against the Cramer Rao Lower Bound (CRLB). Under the Gaussian range measurement error assumption, R-LS is an asymptotically efficient and unbiased estimator as $N \to \infty$, achieving an estimation covariance identical to the Cramer-Rao lower bound (CRLB):

$$\text{CRLB} = \left(\sum_{i=1}^{N} \frac{1}{\sigma_i^2 d_i^2} (\mathbf{p} - \mathbf{p}_i)(\mathbf{p} - \mathbf{p}_i)^T \right)^{-1} \tag{6}$$

where $d_i = \|\mathbf{p} - \mathbf{p}_i\|$ and σ_i is the i$^{\text{th}}$ range noise standard deviation. Even though R-LS is considered to be a benchmark because of its asymptotic efficiency [4], it is neither efficient nor unbiased for finite N.

3. Squared Range Based Estimation Approaches

In this section we focus on source localization approaches based on squared ranges. The main difficulty of finding the LS global minimiser is the presence of the square root operator in the objective function (1). If we square the norm in each term and compare it to the square of its associated measured range, then a polynomial objective function of degree four emerges. A rich repertoire of polynomial and quadratic optimization techniques may then be applied to globally solve the problem. However, the source position estimate is only suboptimal in the maximum likelihood sense. In the following we present and compare two squared range based least squares (SR-LS) estimation techniques.

The basic SR-LS source position estimate is obtained by solving

$$\min_{\mathbf{p}} g(\mathbf{p}) = \sum_{i=1}^{N} w_i \left(\|\mathbf{p} - \mathbf{p}_i\|^2 - \tilde{d}_i^2 \right)^2 \tag{7}$$

where the parameters, w_i, are positive weights. In what follows we will derive a variation of this estimator, which proves to be more optimal in a maximum likelihood sense

3.1 Range Weighted SR-LS

Observe that $g(\mathbf{p})$ in (7) can also be expressed as

$g(\mathbf{p}) = \sum_{i=1}^{N} w_i \left(\|\mathbf{p} - \mathbf{p}_i\| - \tilde{d}_i \right)^2 \left(\|\mathbf{p} - \mathbf{p}_i\| + \tilde{d}_i \right)^2$ and note that when $\mathbf{p}$ is in the vicinity of the estimated source position, we have $\|\mathbf{p} - \mathbf{p}_i\| \approx \tilde{d}_i$ and therefore

$g(\mathbf{p}) \approx \sum_{i=1}^{N} w_i \left(\|\mathbf{p} - \mathbf{p}_i\| - \tilde{d}_i \right)^2 \left(2\tilde{d}_i \right)^2$. Clearly formulation (7) weighs longer measurement ranges significantly more than shorter ones. Cancelling this undesirable effect leads to the balanced formulation

$$\min_{\mathbf{p}} \sum_{i=1}^{N} \frac{w_i}{\tilde{d}_i^2} \left(\|\mathbf{p} - \mathbf{p}_i\|^2 - \tilde{d}_i^2 \right)^2 \tag{8}$$

which is more optimal in a maximum likelihood sense. We denote position estimator (8) as RW-SRLS, which stands for Range Weighted SR-LS. As we shall see later in the computer simulations section (Section 7), the RW-SRLS estimator results in significant improvement in localization accuracy.

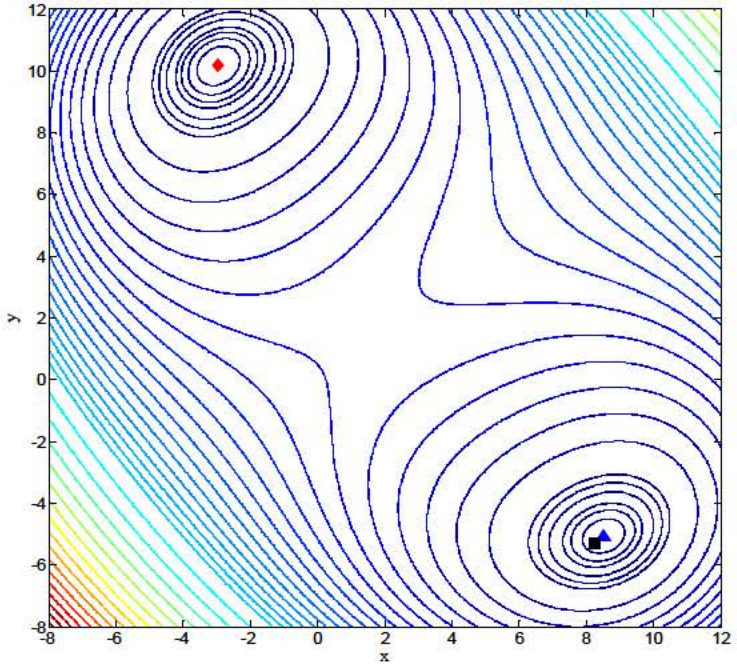

Figure 2: Contour plot of the weighted SR-LS objective function. The global minimum is shown as a red diamond. The blue triangle corresponds to a local minimum. The black square is the true source position.

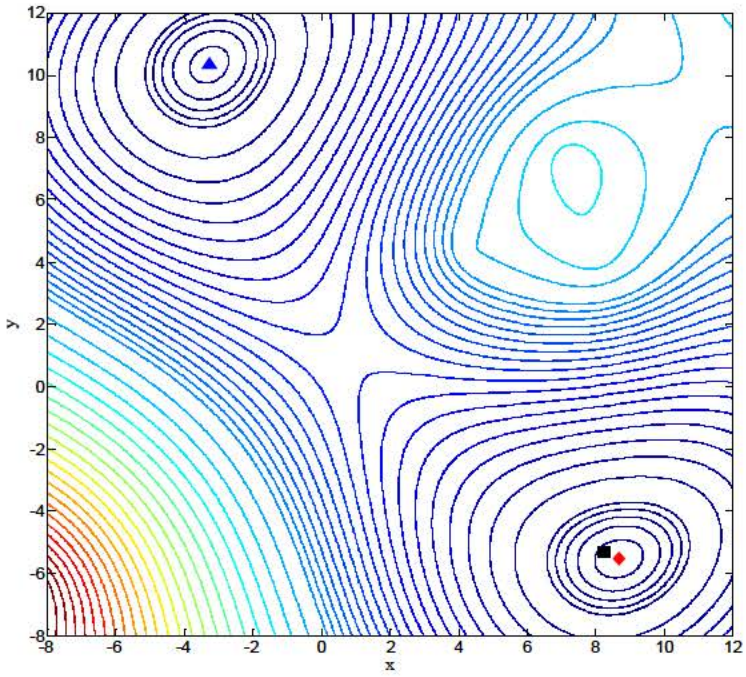

Figure 3: Contour plot of the R-LS objective function. The global minimum is shown as a red diamond. The blue triangle corresponds to a local minimum. The black square is the true source position.

Both the SR-LS and RW-SRLS source position estimation problems are instances of the generalized trust region subproblems (GTRS) [17][18][19]. They are transformed to quadratic optimization problems subject to a single quadratic constraint before being solved. A rigorous application of this approach is given in [3], which includes formulation (7) but not (8). For more details on how to solve (7) or (8), refer to [3][19].

Although (8) is a closer approximation to (1), the R-LS and RW-SRLS global minimisers may occasionally differ considerably. The following numerical example illustrates this point.

Numerical Example: Consider a source located in the plane at position (11.24, -5.32) and assume the availability of 5 sensors whose location coordinates are (7.37, 4.36), (11.00, 4.22), (-8.89, -6.49), (10.20, 7.39) and (-9.84, -6.87). Let the noisy measurements be respectively, 8.45, 11.67, 17.10, 13.32 and 19.81. These are obtained by adding zero mean Gaussian noise of standard deviation ($\sigma = 1.5$) to the true range measurements. Figures 2 and 3 show the contour plots associated with the weighted SR-LS and R-LS objective functions, respectively. The weighted SR-LS global minimum in Figure 2, shown as a red diamond, occurs at (-2.97, 10.19) and has a value of 10.08. The figure also depicts a local minimum (shown as a blue triangle) at (11.52, -5.08) with an objective value of 11.20. Figure 3, on the

other hand, displays an LS global minimum of 10.95 at (11.67, -5.53). The local minimum occurs at (-3.29, 10.35) and has an objective value of 11.21. The two figures demonstrate that the R-LS global minimiser may be very distant from the WR-SRLS global minimiser. In this example the R-LS global minimum occurs in the vicinity of the true source position but this is not always true in general.

4. Geolocation Using Semidefinite Relaxation (SDR)

In the following we present three R-LS approximation algorithms, which are based on the semidefinite relaxation of (1) using different formulation techniques. Solving the relaxed problem is straightforward but the obtained solution may or may not correspond to that of (1). Fortunately a convergence certificate to the global solution of (1) is provided, in the form of a matrix rank test.

4.1 Cheung's Method [7]

This is perhaps the first work which applied convex relaxation techniques to (1). The algorithm details are given in [7] for localization problems in $\Re^2$. However, for more generality and completeness we briefly reproduce this algorithm using notations applicable to both $\Re^2$ and $\Re^3$.

Problem (1) can be equivalently re-expressed as

$$\begin{aligned} \min_{\mathbf{p}, r_i} \quad & f(\mathbf{p}) = \sum_{i=1}^{N} w_i \left(r_i - \tilde{d}_i \right)^2 \\ & r_i^2 = \left\| \mathbf{p} - \mathbf{p}_i \right\|^2, \quad 1 \le i \le N \end{aligned} \tag{9}$$

If we define $\mathbf{G} = \left[r_1, r_2, \cdots, r_N, 1 \right]^T \left[r_1, r_2, \cdots, r_N, 1 \right]$ and $\mathbf{P} = \left[\mathbf{p}^T, 1 \right]^T \left[\mathbf{p}^T, 1 \right] \in \Re^{(n+1)\times(n+1)}$, then (9) may also be formulated equivalently as

$$\begin{aligned} \min_{\mathbf{G}, \mathbf{P}} \quad & \sum_{i=1}^{N} w_i \left(\mathbf{G}_{ii} - 2\mathbf{G}_{N+1\,i}\, \tilde{d}_i + \tilde{d}_i^{\,2} \right) \\ & \mathbf{G}_{ii} = tr\{\mathbf{C}_i\, \mathbf{P}\}, \quad 1 \le i \le N \\ & \begin{bmatrix} \mathbf{G} & 0 \\ 0 & \mathbf{P} \end{bmatrix} \ge 0 \\ & \mathbf{G}_{N+1,\,N+1} = \mathbf{P}_{n+1,\,n+1} = 1 \\ & \operatorname{rank}(\mathbf{G}) = \operatorname{rank}(\mathbf{P}) = 1 \end{aligned} \tag{10}$$

where

$$\mathbf{C}_i = \begin{bmatrix} \mathbf{I} & -\mathbf{p}_i \\ -\mathbf{p}_i & \|\mathbf{p}_i\|^2 \end{bmatrix}$$

By dropping the rank-1 constraint, problem (10) is relaxed to

$$\begin{aligned} \min_{\mathbf{G},\mathbf{P}} \ & \sum_{i=1}^{N} w_i \left(\mathbf{G}_{ii} - 2\mathbf{G}_{N+1\,i}\, \tilde{d}_i + \tilde{d}_i^{\,2} \right) \\ & \mathbf{G}_{ii} = tr\{\mathbf{C}_i \mathbf{P}\}, \quad 1 \le i \le N \\ & \begin{bmatrix} \mathbf{G} & 0 \\ 0 & \mathbf{P} \end{bmatrix} \ge 0 \\ & \mathbf{G}_{N+1,N+1} = \mathbf{P}_{n+1,n+1} = 1 \end{aligned} \tag{11}$$

which can be solved efficiently using interior point methods. It should be pointed out that the global solution of (11) coincides with that of (10) only if the matrices $\mathbf{G}$ and $\mathbf{P}$ are rank-1 (or nearly rank-1 in practice). The solution is extracted from the last column (or row) of $\mathbf{P}$. A recent result due to [3] demonstrated that the solution $\mathbf{G}$ of the relaxed problem is guaranteed to be rank-1. This property, however, does not always carry over to $\mathbf{P}$.

When the solution $\mathbf{P}$ is of rank larger than 1, which is not rare in practice, the global solution to (10) may not be known, but the computed global minimum remains a lower bound to the objective function of (1), (9) or (10). In practice if $\mathbf{P}$ is not of rank 1, a coarse approximate solution to (1) may be obtained by applying the singular value decomposition to $\mathbf{P}$ to find a reduced rank approximation. With more effort one may obtain 'an improved' solution through a randomization process [20]. This is briefly implemented as follows. We first exclude the last column and row of $\mathbf{P}$ and call the resulting submatrix, $\mathbf{P}_e$. We also let $\mathbf{t}$ be the last column of $\mathbf{P}$, without the last entry, '1' . The matrix, $\mathbf{\Sigma} = \mathbf{P}_e - \mathbf{t}\mathbf{t}^T$, is an $n \times n$ error covariance matrix. One may randomly pick $\mathbf{v}$ as a Gaussian random vector from the distribution $\mathbf{v} \sim N(\mathbf{t}, \mathbf{P}_e - \mathbf{t}\mathbf{t}^T)$, because $\mathbf{v}$ solves the optimization problem (9) on average. If enough samples are taken using this distribution, then one may obtain 'an improved' solution for the problem by selecting the sample resulting in the lowest objective value of (1). Alternatively one may be interested in finding a region where the source lies with a given probability, p. The covariance matrix $\mathbf{\Sigma}$ defines an elliptic region given by $(\mathbf{v}-\mathbf{t})^T \mathbf{\Sigma}^{-1} (\mathbf{v}-\mathbf{t}) \le \delta$, where δ controls the size of the elliptic region as a function of p . For a localization problem in the plane, the size parameter, δ , is related to the probability, p , through $\delta = -2\log(1-p)$ [21].

4.2 The SLCP algorithm [12]

The source localization in the complex plane (SLCP) is another semidefinite relaxation program applied to the LS cost function of (1). This program is only

applicable to localization problems in the plane (i.e., $n=2$). Its main approach is to transform the localization problem from $\Re^2$ to the complex plane. Any point on a circle can be represented in the complex domain as $\mathbf{s}_i = \mathbf{p}_i + \tilde{d}_i e^{j\phi_i}$, where $\mathbf{p}_i$ is the circle's centre and $\tilde{d}_i$ its radius. The i[th] point position on the circle is indicated by the phase angle, ϕ_i.

Minimizing the cost function $f(\mathbf{p}) = \sum_{i=1}^{N} w_i \left(\|\mathbf{p} - \mathbf{p}_i\| - \tilde{d}_i \right)^2$ is equivalent to finding the source position closest to the circles in a square sense,

$$\begin{aligned} &\min_{\mathbf{p},\mathbf{s}_i} \sum_{i=1}^{N} w_i \|\mathbf{p} - \mathbf{s}_i\|^2 \\ &\text{subject to} \quad \|\mathbf{p}_i - \mathbf{s}_i\| = \tilde{d}_i \end{aligned} \tag{12}$$

It can be shown [12] that the optimal solution to (12) satisfies $\mathbf{p}^* = \bar{\mathbf{s}} = \sum_{i=1}^{N} w_i \mathbf{s}_i^*$, where $\bar{\mathbf{s}}$ is the weighted average of the optimal circle points, $\mathbf{s}_i^*$.

In the complex domain problem (12) can be re-expressed as

$$\begin{aligned} &\min_{\phi_i} \sum_{i=1}^{N} w_i \|\bar{\mathbf{s}} - \mathbf{s}_i\|^2 \\ &\text{subject to} \quad \mathbf{s}_i = \mathbf{p}_i + \tilde{d}_i e^{j\phi_i} \end{aligned} \tag{13}$$

If we define $\boldsymbol{\theta} = \left[e^{j\phi_1}, e^{j\phi_2}, \ldots, e^{j\phi_N} \right]^T \in C^N$, $\mathbf{a} = \left[p_1, p_2, \ldots, p_N \right]^T \in C^N$, $\mathbf{D} = diag([\tilde{d}_1, \tilde{d}_2, \cdots, \tilde{d}_N]^T)$, $\mathbf{w} = \left[w_1, w_2, \ldots, w_N \right]^T$ and $\boldsymbol{\Sigma} = diag(\mathbf{w}) - \mathbf{w}\mathbf{w}^T$, then (13) becomes

$$\begin{aligned} &\min_{\phi_i} (\mathbf{a} + \mathbf{D}\boldsymbol{\theta})^H \boldsymbol{\Sigma} (\mathbf{a} + \mathbf{D}\boldsymbol{\theta}) \\ &\text{subject to} \quad |\boldsymbol{\theta}| = 1 \end{aligned} \tag{14}$$

Expanding (14) and eliminating constants lead to

$$\begin{aligned} &\min_{\boldsymbol{\theta}} 2\,\mathrm{Re}\{\mathbf{c}^H \boldsymbol{\theta}\} - \boldsymbol{\theta}^H \mathbf{M} \boldsymbol{\theta} \\ &\text{subject to} \quad |\boldsymbol{\theta}| = 1 \end{aligned} \tag{15}$$

where $\mathbf{c}^H = \mathbf{a}^H \Sigma \mathbf{D}$ and $\mathbf{M} = \mathbf{D}\mathbf{w}\mathbf{w}^T\mathbf{D}$

Examining the objective function of (15) we observe that if we substitute $\boldsymbol{\theta}$ by $\boldsymbol{\theta} e^{j\alpha}$, only the linear term, $2\,\mathrm{Re}\{\mathbf{c}^H \boldsymbol{\theta}\}$, changes. This term reaches its minimum of $-2\left|\mathbf{c}^H \boldsymbol{\theta}\right|$ when $\mathbf{c}^H \boldsymbol{\theta}$ becomes real and negative. Hence, problem (15) reduces to

$$\begin{aligned} &\max_{\boldsymbol{\theta}} \; 2\left|\mathbf{c}^H\boldsymbol{\theta}\right| + \boldsymbol{\theta}^H\mathbf{M}\boldsymbol{\theta} \\ &\text{subject to} \quad \left|\boldsymbol{\theta}\right| = 1 \end{aligned} \tag{16}$$

or

$$\begin{aligned} &\max_{\boldsymbol{\theta}} \; 2\sqrt{tr\{\mathbf{c}\mathbf{c}^H\boldsymbol{\theta}\boldsymbol{\theta}^H\}} + tr\{\mathbf{M}\boldsymbol{\theta}\boldsymbol{\theta}^H\} \\ &\text{subject to} \quad \left|\boldsymbol{\theta}\right| = 1 \end{aligned} \tag{17}$$

where the phase vector, $\boldsymbol{\theta}$, is related to that of (16) by a common phase shift.

By putting $\boldsymbol{\Phi} = \boldsymbol{\theta}\boldsymbol{\theta}^H$ and following standard semidefinite programming relaxation techniques, (17) becomes

$$\begin{aligned} &\max_{\boldsymbol{\Phi},t} \; t + tr\{\mathbf{M}\boldsymbol{\Phi}\} \\ &\text{subject to} \quad \boldsymbol{\Phi} \geq 0 \\ &\qquad\qquad \boldsymbol{\Phi}_{ii} = 1 \\ &\qquad\qquad 4tr\{\mathbf{c}\mathbf{c}^H\boldsymbol{\Phi}\} \geq t^2 \end{aligned} \tag{18}$$

which can be solved efficiently using interior point methods. In real form (18) becomes

$$\begin{aligned} &\max_{\mathbf{X},\mathbf{Y},t} \; t + tr\{\mathbf{M}\mathbf{X}\} \\ &\text{subject to} \quad \begin{bmatrix} \mathbf{X} & \mathbf{Y} \\ -\mathbf{Y} & \mathbf{X} \end{bmatrix} \geq 0 \\ &\qquad\qquad \mathbf{X}_{ii} = 1 \\ &\qquad\qquad 4tr\{\mathrm{Re}\{\mathbf{c}\mathbf{c}^H\}\mathbf{X} - \mathrm{Im}\{\mathbf{c}\mathbf{c}^H\}\mathbf{Y}\} \geq t^2 \end{aligned} \tag{19}$$

where $\mathbf{X}$ and $\mathbf{Y}$ (skew-symmetric) correspond to the real and imaginary parts of $\boldsymbol{\Phi}$. The solution may be obtained using singular value decomposition of $\boldsymbol{\Phi}$ (see [12] for more details). It should coincide with that of (1) if the rank of $\boldsymbol{\Phi}$ is 1.

4.3 Closest Point to N Ball Surfaces Problem

In this section we present an improved convex relaxation formulation of the R-LS problem (1), which is applicable to both $\Re^2$ and $\Re^3$. A similar work has also appeared in [13] but we will present our variant convex relaxation of the problem and indicate the differences later in this section.

The gradient at a minimum of (1) is given by (2), where $\mathbf{u}_i = \dfrac{\mathbf{p} - \mathbf{p}_i}{\left\|\mathbf{p} - \mathbf{p}_i\right\|}$ is a unit direction vector pointing from the ith sensor position to the source.

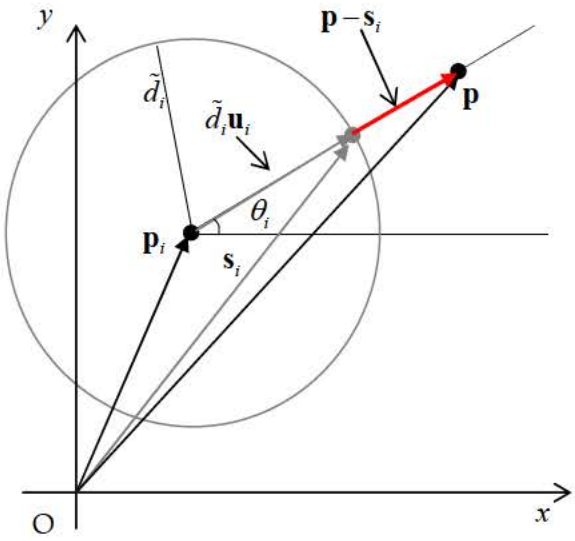

Figure 4: Geometric interpretation of the first order optimality condition in the plane.

If we substitute $\mathbf{s}_i = \mathbf{p}_i + \tilde{d}_i\mathbf{u}_i$ in (2), then from Figure 4 it is clear that each residual error, $\mathbf{p}-\mathbf{s}_i$, is radial to the circle/sphere given by $\|\mathbf{s}_i - \mathbf{p}_i\|^2 - \tilde{d}_i^2 = 0$. This is indeed true because $\mathbf{p}-\mathbf{s}_i = \mathbf{p}-\mathbf{p}_i - \tilde{d}_i\mathbf{u}_i = \left(1 - \frac{\tilde{d}_i}{\|\mathbf{p}-\mathbf{p}_i\|}\right)(\mathbf{p}-\mathbf{p}_i)$. Furthermore the i$^{\text{th}}$ term in the objective function can be re-expressed as a function of the residual error as $\left(\|\mathbf{p}-\mathbf{p}_i\| - \tilde{d}_i\right)^2 = \left\|\left(\|\mathbf{p}-\mathbf{p}_i\| - \tilde{d}_i\right)\mathbf{u}_i\right\|^2 = \left\|\mathbf{p}-\mathbf{p}_i - \tilde{d}_i\mathbf{u}_i\right\|^2 = \|\mathbf{p}-\mathbf{s}_i\|^2$.
In light of this we may write

$$\begin{aligned} &\min_{\mathbf{p},\mathbf{s}_i} \sum_{i=1}^{N} w_i \|\mathbf{p}-\mathbf{s}_i\|^2 \\ &\text{subject to } \|\mathbf{s}_i - \mathbf{p}_i\|^2 = \tilde{d}_i^2 \end{aligned} \tag{20}$$

Problem (20) may be looked at as the problem of finding a point, $\mathbf{p}$ in $\Re^n$, closest in a weighted LS sense to N ball surfaces, $\partial B_{\mathbf{p}_i,d_i}$, $1 \le i \le N$. Hence it is convenient to refer to problem (20) as the closest point to N ball surfaces problem (CPNBSP). Writing down the first optimality condition of (20) with respect to $\mathbf{p}$ results in

$\mathbf{p} = \sum_{k=1}^{N} w_k \mathbf{s}_k$, which shows that the closest point to N ball surfaces is a weighted centroid point of N ball surface points satisfying

$$\begin{aligned} &\min_{\mathbf{u}_i} \sum_{i=1}^{N} w_i \left\| \sum_{k=1}^{N} w_k \mathbf{s}_k - \mathbf{s}_i \right\|^2 \\ &\text{subject to} \quad \mathbf{s}_i = \mathbf{p}_i + \tilde{d}_i \mathbf{u}_i, \\ &\qquad \left\| \mathbf{u}_i \right\|^2 = 1, \; 1 \le i \le N \end{aligned} \tag{21}$$

Clearly both problems (20) and (21) are equivalent and the only difference is that $\mathbf{p}$ is made explicit in (20). A similar expression to (21) appeared in [13]. The unknown variables in (21) are the unit vectors $\mathbf{u}_i$. Expanding $\sum_{i=1}^{N} w_i \left\| \sum_{k=1}^{N} w_k \mathbf{s}_k - \mathbf{s}_i \right\|^2$ results in $\sum_{i=1}^{N} w_i \, \mathbf{s}_i^T \mathbf{s}_i - \sum_{i=1}^{N} \sum_{j=1}^{N} w_i w_j \, \mathbf{s}_i^T \mathbf{s}_j$. If we let $\mathbf{S} = [\mathbf{s}_1, \mathbf{s}_2, \cdots, \mathbf{s}_N]^T$, $\mathbf{w} = [w_1, w_2, \cdots, w_N]^T$ and $\mathbf{\Sigma} = \mathbf{w}\mathbf{w}^T - diag(\mathbf{w})$ then this latter expression can be written compactly as $-tr\left\{\mathbf{S}^T \mathbf{\Sigma} \mathbf{S}\right\}$ where $tr\{.\}$ refers to the trace operator. If we further let $\mathbf{a} = [\mathbf{p}_1, \mathbf{p}_2, \cdots, \mathbf{p}_N]^T$, $\mathbf{D} = diag([\tilde{d}_1, \tilde{d}_2, \cdots, \tilde{d}_N]^T)$ and $\mathbf{U} = \left[\mathbf{u}_1, \mathbf{u}_1, \cdots, \mathbf{u}_N\right]^T$ then from the definition of $\mathbf{s}_i = \mathbf{p}_i + d_i \mathbf{u}_i$ it follows that $\mathbf{S} = \mathbf{a} + \mathbf{D}\mathbf{U}$ and (21) becomes

$$\begin{aligned} &\max_{\mathbf{U}} tr\left\{ (\mathbf{a} + \mathbf{D}\mathbf{U})^T \mathbf{\Sigma} (\mathbf{a} + \mathbf{D}\mathbf{U}) \right\} \\ &\text{subject to} \quad \left|\mathbf{U}\right| = 1 \end{aligned} \tag{22}$$

where $\left|\mathbf{U}\right| = 1$ signifies that each row of $\mathbf{U}$ has a norm of 1. Note that although problem (22) appears similar to (14), formulation (22) is not restricted to localization problems in the plane.

Putting $\mathbf{c} = \mathbf{D}\mathbf{\Sigma}\mathbf{a}$ and $\mathbf{M} = \mathbf{D}\mathbf{w}\mathbf{w}^T\mathbf{D}$ and expanding (22) leads to the optimization problem

$$\begin{aligned} &\max_{\mathbf{U}} tr\left\{ \mathbf{c}^T \mathbf{U} + \mathbf{U}^T \mathbf{c} + \mathbf{U}^T \mathbf{M} \mathbf{U} \right\} \\ &\text{subject to} \quad \left|\mathbf{U}\right| = 1 \end{aligned} \tag{23}$$

Although problem (23) is difficult to solve because it is non-convex, it can be shown that $\mathbf{c}^T\mathbf{U}$ is symmetric, positive semidefinite at an optimal solution. We next consider relaxing formulation (23) to be able to solve it or find an approximate solution to it. Let $\mathbf{T}$ be the augmented n-column matrix formed by appending the

$n \times n$ identity matrix, $\mathbf{I}_n$, to the bottom of $\mathbf{U}$ (i.e. $\mathbf{T} = [\mathbf{U}; \mathbf{I}_n]$). If we form $\mathbf{\Psi} = \mathbf{T}\mathbf{T}^T$, then $\mathbf{\Psi}$ can be partitioned as $\mathbf{\Psi} = \begin{bmatrix} \mathbf{\Phi} & \mathbf{\Theta} \\ \mathbf{\Theta}^T & \mathbf{I}_n \end{bmatrix}$ where $\mathbf{\Phi} = \mathbf{U}\mathbf{U}^T$ and $\mathbf{\Theta} = \mathbf{U}$. The rank of $\mathbf{\Psi}$ is n. The objective function of (23) may be expressed in terms of $\mathbf{\Psi}$ as $tr\{\mathbf{K}\mathbf{\Psi}\}$ where $\mathbf{K} = \begin{bmatrix} \mathbf{M} & \mathbf{c} \\ \mathbf{c}^T & 0_{n \times n} \end{bmatrix}$. Using these notations, the convex relaxation of (23) reads as

$$\begin{aligned} \max_{\mathbf{\Psi}} \quad & tr\{\mathbf{K}\mathbf{\Psi}\} \\ & \mathbf{\Psi} \geq 0, \quad \mathbf{\Psi}_{ii} = 1, \; 1 \leq i \leq N, \\ & \mathbf{\Psi}_{N+1:N+n,\, N+1:N+n} = \mathbf{I}_n \end{aligned} \tag{24}$$

where the non-convex constraint, $\text{rank}(\mathbf{\Psi}) = n$, has been dropped.

Problem (24) can be solved efficiently using interior point methods. Similar to (23), it can be shown that $\mathbf{c}^T\mathbf{\Theta}$ is positive semidefinite at an optimal solution. Let the solution of (24) be $\mathbf{\Psi}^*$. If the rank of $\mathbf{\Psi}^*$ is approximately n then $\mathbf{\Theta}$ is numerically an approximate solution of (23). Set the final solution to $\mathbf{\Theta}^* = \mathbf{\Theta}$. If the rank is larger than n, then an approximate source solution is obtained as follows

1. Compute the singular value decomposition (SVD) of $\mathbf{\Psi}^*$ as $\mathbf{L}\mathbf{\Lambda}\mathbf{R}^T$. The singular values in $\mathbf{\Lambda}$ are arranged in a decreasing order.
2. Extract the diagonal $n \times n$ submatrix, $\overline{\mathbf{\Lambda}}$, consisting of the n largest singular values of $\mathbf{\Psi}^*$ (i.e. the n largest diagonal values of $\mathbf{\Lambda}$). Similarly let $\overline{\mathbf{L}}$ be the n columns of $\mathbf{L}$ associated with the largest n singular values, after removing the bottom n rows. The size of $\overline{\mathbf{L}}$ is $N \times n$. Finally let $\overline{\mathbf{R}}$ be the n columns of $\mathbf{R}$ associated with the largest n singular values and only keeping the bottom n rows. The size of $\overline{\mathbf{R}}$ is $n \times n$.
3. Compute $\overline{\mathbf{L}}\,\overline{\mathbf{\Lambda}}\,\overline{\mathbf{R}}^T$, normalize the rows to 1 and store the outcome in $\mathbf{\Theta}$.
4. Compute the SVD of $\mathbf{A} = \mathbf{c}^T\mathbf{\Theta}$ as $\mathbf{K}\mathbf{\Omega}\mathbf{Q}^T$ and return $\mathbf{\Theta}^* = \mathbf{\Theta}\mathbf{Q}\mathbf{K}^T$.

The estimated source location follows as

$$\mathbf{p}^* = (\mathbf{a} + \mathbf{D}\mathbf{\Theta}^*)^T \mathbf{w} \tag{25}$$

Note that in [13] the authors derived a slightly different SDR problem to (24). The main difference is that our relaxation formulation (24) makes explicit use of $\mathbf{\Theta}$ and $\mathbf{\Phi}$ whereas their formulation (see (16) in [13]), makes use of $\mathbf{\Phi}$ and $\mathbf{Z}$ where $\mathbf{Z}$ is related to $\sqrt{\mathbf{A}\mathbf{A}^T}$. The implication of this is that even if the rank of $\mathbf{\Phi}$ is n, the computed $\mathbf{U}$ (by applying SVD on $\mathbf{\Phi}$) is usually not the problem solution and one

has to adjust $\mathbf{U}$ through application of an optimal orthogonal transformation by executing (12) of [13]. In our work this step is needed only if the rank of $\boldsymbol{\Psi}^*$ is larger than n and is carried out using polar decomposition, which is implemented using SVD.

5. Geolocation Using the Continuation Method [16]

The material presented in this section is mostly based on [16]. For computation purposes we deviate from [16] and provide simplified expressions as a function of the modified Bessel functions and their approximations. The application of the continuation method to the source position estimation problem consists of convolving the original LS objective function with a smoothing kernel before solving the localization problem. The idea is to initially apply excessive smoothing to the extent that the objective function becomes convex. Minimizing a convex function is straightforward to implement as local search techniques such as gradient descent methods become global search methods. By progressively tapering the smoothing effect and solving the problem starting from the solution of the previous step, a final more robust solution is often obtained. If suitable care is applied to the tapering process this progressive optimization method usually results in an accurate approximation of the R-LS solution.

The main issues of this approach are the choice of a smoothing kernel and the derivation of closed form expressions for the smoothed objective function and its gradient. Using the Gaussian kernel, $g(u,\lambda) = e^{-u^2/\lambda^2}$, Destino *et al.* [16] were able to derive expressions for the smoothed objective function and its gradient as

$$f_\lambda(\mathbf{p}) = \sum_{i=1}^{N} w_i f_\lambda^i(\mathbf{p}) = \sum_{i=1}^{N} w_i \left(\tilde{d}_i^2 + r_i^2 + \lambda^2 - \lambda\sqrt{\pi}\tilde{d}_i \, {}_1F_1\left(\frac{3}{2},1,\frac{r_i^2}{\lambda^2}\right) e^{\frac{-r_i^2}{\lambda^2}} \right) \tag{26}$$

and

$$\nabla_{\mathbf{p}} f_\lambda(\mathbf{p}) = \sum_{i=1}^{N} w_i \nabla_{\mathbf{p}} f_\lambda^i(\mathbf{p}) = \sum_{i=1}^{N} w_i s_i'(r_i,\lambda) \frac{\mathbf{p}-\mathbf{p}_i}{\|\mathbf{p}-\mathbf{p}_i\|} \tag{27}$$

where $s_i'(r_i,\lambda) = 2r_i + \sqrt{\pi}\dfrac{\tilde{d}_i r_i}{\lambda} S_1(r_i,\lambda)$ and $S_1(r_i,\lambda) = e^{\frac{-r_i^2}{\lambda^2}}\left(2\,{}_1F_1\left(\frac{3}{2},1,\frac{r_i^2}{\lambda^2}\right) - 3\,{}_1F_1\left(\frac{5}{2},2,\frac{r_i^2}{\lambda^2}\right)\right)$.

The variable, r_i, represent the ith sensor-source Euclidian distance, $\|\mathbf{p}-\mathbf{p}_i\|$, where $\mathbf{p}$ is the unknown source position in $\Re^2$. The function ${}_1F_1(a,b,z)$ is the confluent hypergeometric function. The parameter, $\lambda \geq 0$, controls the amount of smoothing. The larger this parameter is, the more smoothing is applied to the objective

function. As λ approaches zero, the function (26) converges to the original objective function, $f(\mathbf{p})$.

To compute the smoothed objective function and its gradient, we depart from the original derivations given in [16] and take advantage of two useful properties of confluent hypergeometric functions. These are

$$ {}_1F_1\left(\frac{3}{2},1,z\right) = e^{z/2}\left((z+1)I_o(\frac{z}{2}) + zI_1(\frac{z}{2})\right) \tag{28} $$

$$ {}_1F_1\left(\frac{5}{2},2,z\right) = \frac{1}{3}e^{z/2}\left((2z+3)I_o(\frac{z}{2}) + (2z+1)I_1(\frac{z}{2})\right) \tag{29} $$

where $I_o(.)$ and $I_1(.)$ are modified Bessel functions of the first kind of order 0 and 1. Using these two identities, $S_1(r,\lambda)$ reduces to $S_1(r,\lambda) = -e^{-x}\left(I_o(x)+I_1(x)\right)$ where $x = \dfrac{r^2}{2\lambda^2}$.

Now to compute the modified Bessel functions, it is advantageous to make use of polynomial approximations, developed by E. E. Allen [22]. These are

$$ \sqrt{x}e^{-x}I_o(x) = 0.39894228 + 0.013285917t + 0.002253187t^2 $$
$$ -0.001575649t^3 + 0.009162808t^4 - 0.020577063t^5 $$
$$ +0.026355372t^6 - 0.016476329t^7 + 0.003923767t^8 = Q_o(\mathrm{x}) $$
$$ \sqrt{x}e^{-x}I_1(x) = 0.39894228 - 0.039880242t - 0.003620183t^2 $$
$$ +0.001638014t^3 - 0.01031555t^4 + 0.022829673t^5 $$
$$ -0.028953121t^6 + 0.017876535t^7 - 0.004200587t^8 = Q_1(\mathrm{x}) $$

where $t = \dfrac{3.75}{x}$ and x is in the interval $[3.75,+\infty)$. The largest approximation error in this infinite region is $\approx 2.0\times10^{-7}$. This region is of interest when λ approaches zero. The i[th] (unweighted) term in the smoothed objective function is approximated as

$$ \begin{aligned} f_\lambda^i(\mathbf{p}) &= \tilde{d}_i^2 + r_i^2 + \lambda^2 - \sqrt{\pi}\tilde{d}_i r_i \frac{1}{\sqrt{2x_i}} e^{-x_i}\left((2x_i+1)I_o(x) + 2x_i I_1(x_i)\right) \\ &= \tilde{d}_i^2 + r_i^2(1+\frac{1}{2x_i}) - \sqrt{2\pi}\tilde{d}_i r_i\left((1+\frac{1}{2x_i})Q_o(x_i) + Q_1(x_i)\right) \end{aligned} \tag{30a} $$

where $x_i = \dfrac{r_i^2}{2\lambda^2}$ and $x_i > 3.75$. Its corresponding gradient $\nabla_{\mathbf{p}} f_\lambda^i(\mathbf{p})$ becomes approximately

$$ \nabla_{\mathbf{p}} f_\lambda^i(\mathbf{p}) \approx \left(2 - \sqrt{2\pi}\frac{\tilde{d}_i}{r_i}\left(Q_o(x_i) + Q_1(x_i)\right)\right)(\mathbf{p} - \mathbf{p}_i) \tag{30b} $$

For smaller values of x $(0 \le x \le 3.75)$, which correspond to large values of λ, we make use of the following approximations [22]

$$I_o(x)=1+3.5156229t^2+3.0899424t^4+1.2067492t^6$$
$$+0.2659732t^8+0.0360768t^{10}+0.0045813t^{12}$$
$$x^{-1}I_1(x)=0.5+0.87890594t^2+0.51498869t^4+0.15084934t^6$$
$$+0.02658733t^8+0.00301532t^{10}+0.00032411t^{12}$$

where $t=\frac{x}{3.75}$. The approximation errors are less than $\approx 3.0\times10^{-8}$ for $I_o(x)$ and $\approx 1.0\times10^{-8}$ for $I_1(x)$. In this region, the i[th] (unweighted) term of the smoothed objective function becomes

$$f_\lambda^i(\mathbf{p})=\tilde{d}_i^2+r_i^2(1+\frac{1}{2x_i})-\sqrt{\pi}\,\tilde{d}_i r_i\frac{1}{\sqrt{2x_i}}e^{-x_i}\left((2x_i+1)I_o(x_i)+2x_i\,I_1(x_i)\right) \quad (31a)$$

and its gradient reduces to

$$\nabla_{\mathbf{p}} f_\lambda^i(\mathbf{p})=\left(2-\sqrt{2\pi}\frac{\tilde{d}_i}{r_i}\sqrt{x_i}\,e^{-x_i}\left(I_o(x_i)+I_1(x_i)\right)\right)(\mathbf{p}-\mathbf{p}_i) \quad (31b)$$

where $x_i=\frac{r_i^2}{2\lambda^2}$ and $0<x_i\le 3.75$.

Destino *et al.* [16] have derived an expression for a starting initial value for the smoothing parameter, λ, that ensures the convexity of $f_\lambda(\mathbf{p})$. This value is

$$\lambda_o=\frac{\sqrt{\pi}}{2}\max_{1\le i\le N}\{\tilde{d}_i\} \quad (32)$$

Starting from λ_o and an arbitrary initial source position estimate, $\mathbf{p}_o$, a practical gradient descent algorithm would converge to the global minimum because $f_{\lambda_o}(\mathbf{p})$ is convex by construction. This global solution becomes the starting point for the next gradient descent iteration where λ is stepped down to a new value. By progressively reducing the value of λ in discrete steps and solving the localization problem starting from the solution of the previous step, a succession of more accurate solution updates are usually obtained. The main aim of this solution method is to steer the final solution towards the global minimum of the original cost function $f(\mathbf{p})$. As argued in [16] this is almost always achieved after a few fixed iterations of λ. In our computer simulations we reduced λ according to the geometric progression law, $\lambda_k=\lambda_o\,0.6^k$, with $k=0,1,2,\cdots,10$ and added a last iteration where $\lambda=0$, resulting in a total of 12 iterations.

6. Geolocation Using the Null Space Method

In this section we focus on applying Reid and Zhi's method [10] (or RZ for short) to solve systems of polynomial equations with finitely many solutions (i.e. zero-dimensional polynomial systems). We have selected to use RZ because of its simplicity and efficiency to solve this problem. Although this method solves exactly the polynomial system associated with (1) for an arbitrary, N, it becomes computationally prohibitive and inaccurate as N increases beyond 3, which coincides with the minimum number of measurements required to generate an unambiguous source position solution in the plane.

Referring to Figure 5 and substituting $\mathbf{u}_i = [\cos\theta_i, \sin\theta_i]^T$ in (3) and expanding, we obtain

$$\begin{cases} x = A + \sum_{i=1}^{N} w_i \tilde{d}_i \cos\theta_i \\ y = B + \sum_{i=1}^{N} w_i \tilde{d}_i \sin\theta_i \end{cases} \tag{33}$$

where $\mathbf{p} = [x\ y]^T$, $A = \sum_{i=1}^{N} w_i x_i$ and $B = \sum_{i=1}^{N} w_i y_i$.

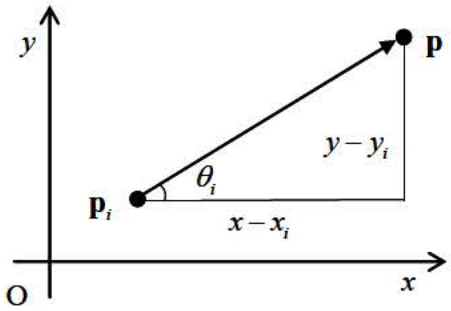

Figure 5: Relationship between $\mathbf{p} - \mathbf{p}_i$ *and bearing angle* θ_i

From Figure 5 it also follows that $\cos\theta_i\,(y - y_i) = \sin\theta_i\,(x - x_i)$, which leads to N trigonometric equations of N unknown angles,

$$(B - y_j)\cos\theta_j + (x_j - A)\sin\theta_j + \sum_{i=1}^{N} w_i \tilde{d}_i \sin(\theta_i - \theta_j) = 0,\ (1 \le j \le N) \tag{34}$$

When the number of sensors is restricted to N=3, then applying (34) for each bearing angle leads to a system of three trigonometric equations of three variables. By applying the normalization property, $c_i^2 + s_i^2 = 1$, where c_i and s_i stand for $\cos\theta_i$ and $\sin\theta_i$, we obtain the equivalent polynomial system

$$
\begin{aligned}
&(B-y_1)\,\mathrm{c}_1+(x_1-A)\,\mathrm{s}_1+w_2\tilde{d}_2(s_2c_1-c_2s_1)+w_3\tilde{d}_3(s_3c_1-c_3s_1)=0,\quad c_1^2+s_1^2-1=0\\
&(B-y_2)\,\mathrm{c}_2+(x_2-A)\,\mathrm{s}_2+w_1\tilde{d}_1(s_1c_2-c_1s_2)+w_3\tilde{d}_3(s_3c_2-c_3s_2)=0,\quad c_2^2+s_2^2-1=0\\
&(B-y_3)\,\mathrm{c}_3+(x_3-A)\,\mathrm{s}_3+w_1\tilde{d}_1(s_1c_3-c_1s_3)+w_2\tilde{d}_2(s_2c_3-c_2s_3)=0,\quad c_3^2+s_3^2-1=0
\end{aligned}
\qquad (35)
$$

which can be solved using a number of polynomial system solving techniques [8][9][10]. An upper bound solution count for this system is $2^6=64$. Using Groebner based analysis the solution count is only 20.

In the following we briefly review Reid and Zhi's method [10] for solving polynomial systems and provide an algorithm that exactly solves (35), subject only to numerical round-off errors. A polynomial system, $\mathbf{S}$, in $\Re[x_1,x_2,\cdots,x_m]$ of degree q may be written in matrix form as $\mathbf{M}_q\mathbf{x}_q=0$ where $\mathbf{x}_q=\left[x_1^q,x_1^{q-1}x_2,...,x_m^2,x_1,...,x_m,1\right]$. In our localization problem $\mathbf{S}$ consists of the six polynomials given in (35). The number of variables is $m=6$ and the system's degree is $q=2$. The main idea behind the RZ method is to expand the polynomial set, $\mathbf{S}$, by multiplying each polynomial of $\mathbf{S}$ by monomials up to some total degree, which is determined by the involutive criterion for zero-dimensional polynomial systems [10]. The process of expanding $\mathbf{S}$ is achieved through prolongation [10]. A single prolongation of $\mathbf{S}$ increases the system's largest total degree by one. Prolongations up to an order *k* result in the polynomial system, $\mathbf{S}^{(k)}$, which can be represented in matrix form as, $\mathbf{M}_t\mathbf{x}_t=0$, where the non-zero entries of $\mathbf{M}_t$ consist of shifted polynomial coefficients of $\mathbf{S}$ and the total degree, *t*, is related to prolongation order, *k*, through $t=q+k$. The vector, $\mathbf{x}_t$, stacks all monomials up to total degree, *t*. Clearly all solutions reside in the null space of $\mathbf{M}_t$ for all $t\geq q$. The null space is represented in matrix form as $\mathbf{B}_t$ where the columns constitute a null space basis of $\mathbf{M}_t$.

In addition to the prolongation operator Reid and Zhi defined the projection operator which is applied to null space bases. A single projection involves removing rows of $\mathbf{B}_t$ associated with the total degree, *t*. This projection step, denoted as $\pi(\mathbf{S}^{(k)})$ has the effect of reducing the total degree of $\mathbf{x}_t$ by one, hence mapping $\mathbf{x}_t$ into $\mathbf{x}_{t-1}$. Higher order projections are represented as $\pi^\ell(\mathbf{S}^{(k)})$ where ℓ is the projection order ($0\leq\ell\leq k$). The main result of the involutive criterion is that one seeks the smallest prolongation order, *k*, such that there exists a projection order, ℓ, satisfying

$$
\dim\pi^\ell(\mathbf{S}^{(k)})=\dim\pi^{\ell+1}(\mathbf{S}^{(k)})=\dim\pi^{\ell+1}(\mathbf{S}^{(k+1)}) \qquad (36)
$$

where dim denotes space dimension. If for a given order, *k*, more than one ℓ satisfies this relationship, then we select the largest projection order ℓ [10]. The common dimension corresponds to the number of solutions of $\mathbf{S}$.

Table I: Reid and Zhi's Algorithm (Null Space Method) [10]

1. Construct the expanded sparse matrix, $\mathbf{M}_t$, where t corresponds to the involution criterion degree.
2. Compute the null space of $\mathbf{M}_t$ and stack its basis along the columns of $\mathbf{B}_t$.
3. Perform ℓ and $\ell+1$ projections on $\mathbf{B}_t$. In other words, keep rows associated with monomials up to total degree $t-\ell$ and $t-\ell-1$ and call the resulting matrices $\mathbf{B}$ and $\mathbf{B}_1$, respectively.
4. Compute the SVD of $\mathbf{B}_1 = [\mathbf{U}_1 \;\; \mathbf{U}_2] \cdot [\mathbf{\Sigma}_1 \;\; \mathbf{0}]^T \cdot \mathbf{V}^T$
5. Form the multiplication matrix, $\mathbf{M}_{x_i}$, with respect to a selected variable, x_i, using $\mathbf{M}_{x_i} = \mathbf{U}_1^T \cdot \mathbf{B}_{x_i} \cdot \mathbf{V} \cdot \mathbf{\Sigma}_1^{-1}$ where $\mathbf{B}_{x_i}$ consists of rows of $\mathbf{B}$ corresponding to the monomials $x_i \cdot \mathbf{x}_{t-l-1}$.
6. Compute the eigenvectors, $\mathbf{v}_j$, of $\mathbf{M}_{x_i}$ and recover all solutions of $\mathbf{S}$ from the entries of $\mathbf{U}_1 \mathbf{v}_j$ in $\mathbf{x}_{t-l-1}$ (after proper scaling)
7. If the polynomial system, $\mathbf{S}$, is the result of a real polynomial optimization, then select the globally optimal real solutions

Table II: Dimension of $\pi^\ell(\mathbf{S}^{(k)})$

N=3	k=2 (t=4)	k=3 (t =5)	k=4 (t =6)	k=5 (t =7)
ℓ=0	57	63	76	92
ℓ=1	26	**21**	20	20
ℓ=2	16	**21**	**20**	20
ℓ=3	6	16	**20**	**20**
ℓ=4	1	6	16	20
ℓ=5	0	1	6	16
ℓ=6	0	0	1	6
ℓ=7	0	0	0	1

Once the prolongation and projection orders associated with involution are known, Reid and Zhi have shown how to construct a multiplication matrix, $\mathbf{M}_{x_i}$, with respect to a given variable, x_i, and apply eigen-decomposition to determine the

solutions of $\mathbf{S}$. It turns out that the multiplication matrix can be generated from knowledge of $\mathbf{B}_t$. The algorithm to compute this matrix is detailed in Table I.

Table II shows the dimension of $\pi^{\ell}(\mathbf{S}^{(k)})$ for our polynomial system (35), for different prolongation and projection orders. The first row gives the dimension of the null space of the expanded matrix, $\mathbf{M}_t$. The involutive condition (36) is satisfied at $t=6$ $(k=4)$ and $\ell=2$ as indicated by the boldface entries in the table. The number of solutions is 20. The size of the expanded matrix, $\mathbf{M}_{t=6}$, is 1260×924, which is rather large to efficiently compute the solutions of (35). If we instead consider column $t=5$ in the table, we observe that $\dim \pi(\mathbf{S}^{(3)}) = \dim \pi^2(\mathbf{S}^{(3)}) = 21$. The associated expanded matrix $\mathbf{M}_{t=5}$ is of much reduced size (504×462), allowing a much faster application of the algorithm.

Running the algorithm on a PC equipped with Intel(R) Core(TM)i7-2600 CPU @ 3.40 GHz, takes about 0.03s to find the global minimum of (1). For a larger number of range measurements ($N \geq 4$), solving (34) is in principle possible, but proves to be impractical using the RZ method because it scales poorly with the number of measurements. Other polynomial solution methods also suffer for larger N. However, the computational complexity of some grows much faster than others. As an example we have applied the polyhedral homotopy method [8] to the N=3 and N=4 localization problems, and it took 0.09s and 0.5s to respectively solve them (20 solutions for N=3 and 64 solutions for N=4). In comparison, the RZ method resulted, on average, in 0.03s and 13s, respectively.

7. Computer Simulations

This section provides a comparative performance analysis in the plane in terms of source localization accuracy and processing speed for the position estimators presented in this paper. The R-LS estimator is implemented using exhaustive grid search. The purpose of this analysis is to distinguish those estimators having desirable properties such as low computational effort and high localization accuracy.

All computer simulations are conducted in Matlab using a total of 5000 realizations for each experiment. Each experiment consists of fixing the range measurement standard deviation, σ, and randomly selecting sensor and source positions within a square of 20 by 20 length units. This allows us to have a fair comparison between the algorithms regardless of geometry. The range measurements are computed as true Euclidean distances plus zero-mean Gaussian errors with standard deviation,

σ. This setup enables us to compute an average mean square error (MSE) for each estimator across the same 5000 sensor/source positions and noise realizations.

Table 1 provides MSE results for the simulated source localization estimators as a function of the measurement standard deviation error, σ. Four values for σ were chosen as shown in the table. The number of sensors is fixed to 5. As is clear from the table, the MSE of SR-LS is consistently larger than the MSE of the remaining estimators. The R-LS estimator performs best for small measurement errors. For larger measurement errors, the CPNBSP-SDR accuracy is clearly superior to those of all estimators, including R-LS. The range weighted SR-LS is of particular interest as it displays acceptable localization accuracy yet low computational effort.

Table 1: Mean square error as a function of range measurement error, σ, for N=5. Also included are indicative processing times in milliseconds using a PC with Intel(R) Core(TM)2 Duo @ 2.53GHz and 4GB of RAM

N=5	SR-LS (2ms)	RW-SRLS (2ms)	SDR (90ms)	SLCP (190ms)	CPNBSP SDR (70ms)	Contin. (135ms)	R-LS
σ=0.01	2.0e-4	1.4e-4	2.6e-4	1.6e-4	1.8e-4	1.4e-4	1.4e-4
σ=0.1	0.0199	0.0137	0.0308	0.0170	0.0177	0.0501	0.0137
σ=1.0	2.7874	2.0547	2.4247	2.1213	2.0158	2.1574	2.1117
σ=2.0	11.577	10.198	9.3889	9.9240	9.1428	10.126	9.7469

To have an appreciation of how nonlinear localization approaches compare with linear ones, we have also implemented the BLUE estimator (Best linear unbiased estimator [4][23]) whose average MSE results are: 5.6e-4, 0.051, 5.32 and 18.98 for σ=0.01, 0.1, 1.0 and 2.0, respectively. Despite its simplicity and very low average processing time (≈0.23ms), it is clearly a poor localization estimator. Indicative processing time averages are also included in Table 1 to highlight computational effort. Notice that the CPNBSP SDR exhibits the lowest computational effort among all relaxation algorithms.

Table 2: Mean square error as a function of range measurement error, σ, for N=10

N=10	SR-LS	RW-SRLS	SDR	SLCP	CPNBSP SDR	Contin.	R-LS
σ=0.01	8.2e-5	5.1e-5	6.3e-5	5.2e-5	5.4e-5	5.1e-5	5.1e-5
σ=0.1	0.0081	0.0052	0.0063	0.0053	0.0054	0.0052	0.0052
σ=1.0	0.8108	0.5916	0.6361	0.5521	0.5551	0.5413	0.5413
σ=2.0	3.3730	2.8998	2.6818	2.4003	2.3759	2.3404	2.3446

Table 2 provides MSE results for *N*=10. The SR-LS provides the worst localization accuracy performance. The R-LS and the continuation method appear to be the most accurate estimators. The SLCP and CPNBSP SDR accuracy performances come next and are close approximations to R-LS. The CPNBSP SDR's computational efficiency is moderate (≈95ms). The weighted SR-LS offers a slightly degraded accuracy but a much lower computation time (≈2.1ms), making it an attractive estimator for practical use.

The next set of computer simulations aim at comparing source localization performances for fixed sensor and emitter positions. Table 3 displays the MSE of six estimators using a fixed scenario of 5 sensors positioned at (6, 4), (0, -8), (-7, 3), (8, -5), (3, -3). The true source location is maintained at (-2, 3). The MSE associated with the Cramer-Rao Lower Bound (CRLB) is depicted in the last column.

Table 3: Mean square error as a function of range measurement error, σ, for a fixed scenario of 5 sensors. The last column shows the lowest achievable MSE

N=5	SR-LS	RW-SRLS	SLCP	CPNBSP SDR	Contin.	R-LS	CRLB
σ=0.01	1.2e-4	1.0e-4	1.0e-4	1.0e-4	1.0e-4	1.0e-4	1.0e-4
σ=0.1	0.0125	0.0102	0.0104	0.0102	0.0102	0.0102	0.0102
σ=1.0	1.2697	1.0769	1.0654	1.0563	1.0512	1.0512	1.0212
σ=2.0	5.1984	4.7314	4.4505	4.4720	4.6983	4.6983	4.0847

As is clear from Table 3, the R-LS performance approaches the CRLB for relatively small distance measurement errors. It clearly departs from CRLB at σ=2.0.

Table 4: Mean square error as a function of range measurement error, σ, for *N*=3

	MSE			Relative MSE	
Range error	R-LS	CPNBSP SDR	SDR [7]	CPNBSP SDR	SDR[7]
σ=0.01	0.176	0.192	0.21	0.027	0.05
σ=0.1	2.152	2.103	2.14	0.27	0.515
σ=1.0	23.84	21.78	21.03	1.373	3.019
σ=2.0	45.83	43.11	41.16	2.016	4.343

Table 4 provides MSE results when *N* is restricted to 3. Four values for σ were chosen as shown in the table. The R-LS position estimator is computed using RZ method as detailed in section 6. For very small range measurement errors, the R-

LS estimator performs best. For large measurement errors, the accuracy of the SDR algorithm [7] is marginally superior to that of CPNBSP SDR. The last two columns in the table show relative MSE with respect to R-LS estimates (i.e., $E\left\{\left\|\mathbf{p}_{CPNBSP\ SDR}-\mathbf{p}_{R-LS}\right\|^2\right\}$ and $E\left\{\left\|\mathbf{p}_{SDR}-\mathbf{p}_{R-LS}\right\|^2\right\}$) and clearly highlight the superior approximation accuracy of the CPNBSP SDR to R-LS.

To summarize, there is not much to gain from the SLCP estimator as its MSE performance is comparable to that of CPNBSP SDR but its computational effort is larger. The SDR estimator is generally less accurate than CPNBSP SDR. The SR-LS is the least accurate estimator. The continuation method can be useful but its performance is less reliable. Its major drawback is that it does not provide a convergence certificate to the global minimum. Grid search R-LS is not practical and does not guarantee convergence to the global minimum. The RZ method provides an exact R-LS solution and is reasonably fast for small localization problems where $N=3$. To conclude it appears that both the CPNBSP SDR and the weighted range SR-LS are the preferred estimators for arbitrary, *N*. Both may also be used for source localization in $\Re^3$. For time critical applications the range weighted SR-LS is obviously the position estimator of choice as it offers the best compromise between estimation accuracy and computational effort.

8. Conclusions

This report presents a review of range-only localization algorithms that aim to approximate the asymptotically efficient but computationally demanding maximum likelihood estimator, which reduces to R-LS if the range measurement errors are normally distributed.

The optimization criteria employed by the range-only localization algorithms cover semidefinite relaxation, global continuation, computer algebra and the generalized trust region subproblem method. Extensive computer simulations were implemented to compare not only the estimation performance of the different algorithms, but also their computational effort. The new proposed algorithms presented in this paper were observed to perform well. The RW-SRLS estimator is suitable for real-time applications. Its accuracy is only slightly worse than that of R-LS. The CPNBSP SDR algorithm, comes second in terms of computational effort but achieves an improved MSE performance, which usually matches that of R-LS. The CPNBSP SDR seems to slightly outperform R-LS in scenarios where only a small number of measurements are available or the measurement errors are large.

9. References

1. R. A. Poisel, *Electronic Warfare Target Location Methods*, Norwood, MA: Artech House, 2005

2. K. W. Cheung, H. C. So, W.-K. Ma and Y. T. Chan, "A Constrained Least Squares Approach to Mobile Positioning: Algorithms and Optimality", *Eurasip Journal on Applied Signal Processing*, pp 1-23, 2006

3. A. Beck, P. Stoica and L. Jian,, "Exact and Approximate Solutions of Source Localization Problems", *IEEE Transactions on Signal Processing,* Vol. 56, no.5, pp.1770-1778, May 2008

4. I. Guvenc and C.-C. Chong, "A survey on TOA based wireless localization and NLOS mitigation techniques," *IEEE Communications Surveys and Tutorials*, Vol. 11, no. 3, pp. 107-124, 2009

5. A.N. Bishop, B. Fidan, K. Dogancay, B.D.O. Anderson, and P.N. Pathirana, "Exploiting geometry for improved hybrid AOA/TDOA-based localization", *Signal Processing*, Vol. 88, pp. 1775-1791, 2008

6. K.W.K. Lui, F.K.W. Chan, and H.C. So, "Accurate time delay estimation based passive localization", *Signal Processing*, Vol. 89, pp. 1835-1838, 2009

7. K. W. Cheung, W. K. Ma, and H. C. So, "Accurate approximation algorithm for TOA-based maximum likelihood mobile location using semidefinite programming," *Proc. ICASSP*, Vol. 2, pp.145–148, 2004

8. A. J. Sommese and C. W. Wampler, The Numerical Solution of Systems of Polynomials Arising in Engineering and Science, World Scientific, Singapore 2005

9. D. Cox, J. Little and D. O'Shea, *Using Algebraic Geometry*, Graduate Texts in Mathematics, Second Edition, Springer 2005

10. G. Reid and L. Zhi, "Solving polynomial systems via symbolic-numeric reduction to geometric involutive form", Journal of Symbolic Computation, Vol. 44, pp. 280-291, 2009

11. S. Boyd and L. Vandenberghe, *Convex Optimization*, Cambridge University Press, 2004

12. P. Ogŭz-Ekim, J. Gomes, J. Xavier and P. Oliveira, "A convex relaxation for approximate maximum-likelihood 2D source localization from range measurements", *IEEE International Conference on Acoustics Speech and Signal Processing (ICASSP),* 14-19, pp.2698-2701, March 2010

13. P. Oğuz-Ekim, J. Gomes et al., "An angular approach for range-based approximate maximum likelihood source localization through convex relaxation", *IEEE Transactions on Wireless Communications*, 2014

14. J. Lasserre, "Global optimization with polynomials and the problem of moments," *SIAM Journal on Optimization*, Vol. 11, pp. 796–817, 2001

15. J. J. Moré and Z. Wu, "Global continuation for distance geometry problems", *SIAM J. on Optimization.*, Vol. 7, pp. 814–836, 1997

16. G. Destino and G.T.F. de Abreu, "Solving the Source Localization Problem via Global Distance Continuation", *IEEE International Conference on Communications Workshops*, pp.1-6, 14-18 June 2009

17. J. J. Moré, "Generalizations of the trust region subproblem", *Optimization Methods and Software*, Vol. 2, pp. 189–209, 1993

18. J. Hiriart-Urruty, "Conditions for Global Optimality 2", *Journal of Global Optimization*, Vol. 13, pp 349-367, 1998

19. J. Nocedal and S Wright, *Numerical Optimization*, Springer Verlag, 2006

20. Z. Luo et al., "Semidefinite Relaxation of Quadratic Optimization Problems", *IEEE Signal Processing Magazine*, Vol. 27, pp 20-34, May 2010

21. D. J. Torrieri, "Statistical Theory of Passive Location Systems", *IEEE Transactions on Aerospace and Electronic Systems*, Vol. 20, pp 183-198, 1984

22. E. E. Allen, "Polynomial approximations to some modified Bessel functions", Mathematical Tables Aids Computation, Vol. 10, pp 162-164, 1956

23. F.K.W. Chan *et al.*, "Best linear unbiased estimator approach for time-of-arrival based localization", *IET Signal Processing*, Vol. 2, No. 2, pp. 156–162, 2008

DEFENCE SCIENCE AND TECHNOLOGY GROUP
DOCUMENT CONTROL DATA

1. DLM/CAVEAT (OF DOCUMENT)

2. TITLE

Recent Advances in Source Localisation Using Range Measurements

3. SECURITY CLASSIFICATION (FOR UNCLASSIFIED REPORTS THAT ARE LIMITED RELEASE USE (L) NEXT TO DOCUMENT CLASSIFICATION)

Document	(U)
Title	(U)
Abstract	(U)

4. AUTHOR(S)

Hatem Hmam and Kutluyil Dogancay

5. CORPORATE AUTHOR

PO Box 1500
Edinburgh South Australia 5111 Australia

6a. DST NUMBER	6b. AR NUMBER	6c. TYPE OF REPORT	7. DOCUMENT DATE
DST-Group-TR-3158	AR-016-408	Technical Report	October 2015

8. FILE NUMBER	9. TASK NUMBER	10. TASK SPONSOR	11. NO. OF PAGES	12. NO. OF REFERENCES
2014/1181114/1	07/308	VCDF	26	23

13. DST Publications Repository

http://dspace.dsto.defence.gov.au/dspace/

14. RELEASE AUTHORITY

Chief, Cyber and Electronic Warfare Division

15. SECONDARY RELEASE STATEMENT OF THIS DOCUMENT

Approved for public release

OVERSEAS ENQUIRIES OUTSIDE STATED LIMITATIONS SHOULD BE REFERRED THROUGH DOCUMENT EXCHANGE, PO BOX 1500, EDINBURGH, SA 5111

16. DELIBERATE ANNOUNCEMENT

No Limitations

17. CITATION IN OTHER DOCUMENTS Yes

18. DST RESEARCH LIBRARY THESAURUS

Time of arrival; Time difference of arrival; Geolocation; Frequency difference of arrival

19. ABSTRACT

In this report we review and present a performance comparison of a number of recently proposed range-based source localization algorithms that approximate the maximum likelihood estimator. Although most of these algorithms are available in the literature we give an elaborated presentation of them and provide some comments on their performances. The optimization techniques used in these localization methods range from convex relaxation, global continuation to the generalized trust region subproblem method. Among the localization algorithms considered, the range weighted squared range least squares estimator (RW-SRLS) seems to be a particularly attractive algorithm as it is fast and yet only marginally suboptimal in a maximum likelihood sense, especially for small range measurement errors.